

DESIGN APPROACH FOR HYBRID ELECTRIC PROPULSION CONCEPTS OF MID-RANGE AIRCRAFT INCLUDING SUSTAINABLE AVIATION FUELS

Karl Ziaja¹, Daniel Lieder², Jan Göing², Jens Friedrichs² & Francesca di Mare¹

¹Ruhr University Bochum, Chair of Thermal Turbomachines and Aeroengines, Bochum 44801, Germany ²Technische Universität Braunschweig, Institute of Jet Propulsion and Turbomachinery, Braunschweig 38092, Germany

Abstract

The aviation industry is facing an urgent need to address the environmental impact of air traffic. This is underlined by the Flightpath 2050 agenda of policymakers and the aerospace industry, which has the ambitious goals of reducing CO_2 emissions by 75 %, NO_x emissions by 90 %, and noise emissions by 65 % until 2050 compared to typical capabilities of new aircraft in 2000. Various technologies are promising solutions to tackle these goals; for example, efficient propulsion concepts, such as Distributed Hybrid Electric Propulsion (DHEP), allow the reduction or even elimination of pollutant emissions through full-electrical operation at ground levels (< 900 m). Another promising option is the use of Sustainable Aviation Fuel (SAF) to reduce chemical emissions directly at the source. This study takes up the potential of DHEP and SAF operation, introducing a design approach for hybrid electric powertrains of mid-range aircraft based on the 0D in-house tool ASTOR for the thermodynamic cycle performance calculation of gas turbines. It has been adapted for on-design calculations and extended by a combustion chamber model to enable the determination of combustion emissions of SAFs. Two approaches, 0D-chemical equilibrium (CE) and 0D-chemical reaction network (CRN), were employed to model the emissions of the combustion process and integrated into the hybrid electric powertrain model using lookup tables. The hybrid electric powertrain model represents a propeller-based DHEP architecture, the gas turbine consisting of a compressor and turbine, as well as the combustion chamber. Appropriate boundary conditions are applied to investigate different propeller-based DHEP concepts. Subsequently, a Design of Experiments-based (DoE) design process is conducted for the SAF powered gas turbine of the hybrid electric powertrain for take-off conidtions providing insights into power-specific fuel consumption (PSFC) and chemical emissions, offering a database enabling new assessments of air pollution at ground level and a pollution driven design selection.

Keywords: Design, Hybrid Electric, Propulsion, Sustainable Aviation Fuels, SAF, Combustion, Emissions

1. Introduction

The aviation sector, with its expansive global footprint, plays a pivotal role in contemporary transportation systems, contributing to approximately 2-3 % of total global carbon dioxide (CO₂) emissions and around 5 % of the overall effective radiative forcing (ERF) impact on the climate ([1]), as a result of other combustion products (e.g., CO₂, H₂O₁, NO_x and soot particles) and condensation trails (contrails). With regards to slowing down climate change, the European Union aims to cut emissions. This is underlined by the Flightpath 2050 agenda ([1, 2]) of policymakers and the aerospace industry, which has the ambitious goals of reducing CO₂ emissions by 75 %, NO_x emissions by 90 % and noise emissions by 65 % until 2050 compared to typical capabilities of new aircraft in 2000. Moreover, recent reports and studies predict a significant growth in air traffic in the EU by 44 % from 2019 until 2050, associated with an increase in pollutant and noise emissions ([3]). These forecasts further emphasize the importance of reducing local pollutant and noise emissions, which pose a direct threat to the health of communities living near airports. EUROCONTROL statistics show that around 0.4 % of all annual deaths are due to a deterioration in air quality, underlining the urgent need for decisive action ([4, 5]). Among the aircraft classes, mid-range aircraft are primarily responsible for pollutant and noise emissions, which account for more than 50 % of the cumulative impact and therefore represent a great potential for improvement. In response to increased concentrations of pollutant emissions in the air, various technologies show promise. For instance, more efficient propulsion concepts, such as Distributed Hybrid Electric Propulsion (DHEP), allow the reduction of pollutant emissions or even their elimination through full-electrical operation at ground levels (< 900 m). Another promising option is the use of Sustainable Aviation Fuel (SAF) to reduce chemical emissions directly at the source. SAFs are a type of Alternative Aviation Fuels (AAF), commonly categorised by hydrotreated ester and fatty acids (HEFA), Alcohol-to-Jet (AtJ), and Fischer-Tropsch (FT) fuels with respect to the production process, that are certified by ICAO for sustainability under the Carbon Offsetting and Reduction Scheme for International Aviation (CORSIA). CORSIA-certified SAFs aim to reduce net Greenhouse gas (GHG) emissions by at least 10 % based on a lifecycle assessment (LCA) for conventional fossil aviation fuels, lowering emissions from 89 g_{CO2}/MJ to 80.1 g_{CO2}/MJ [6]. The potential emissions reduction for different types of SAFs relative to the CORSIA emission criteria are given in Table 1.

Table 1 – Potential LCA based emission reductions compared to the fossil fuel reference value of 89 g_{CO2}/MJ according to [7].

SAF Type	Potential LCA emissions reduction in %	Comment
HEFA	35 - 85	depending on feedstock
FT	85 - 95	based on woody crops and 0 % non-biogenic carbon
AtJ	28 - 73 39 - 73	based on ethanol based on iso-butanol

Despite the high emission reduction potential of SAFs, those based on biomass from carbon-rich stocks (forests, wetlands, peatlands) and areas with high biodiversity should be avoided to prevent

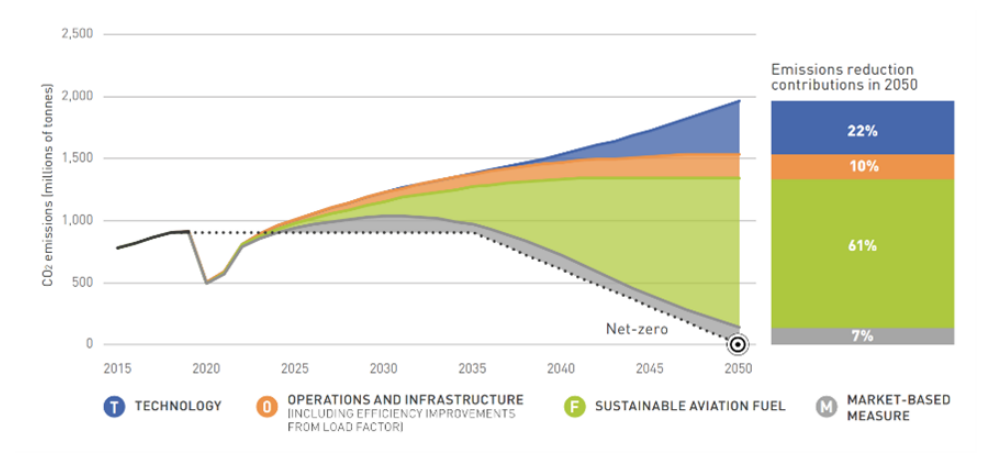


Figure 1 – Potential for carbon reduction until 2050 of various technologies [8].

competition with food and water sources to meet the CORSIA criteria. In addition, dedicated land use for SAF production has an indirect impact on global emissions, which is accounted for by the indirect Land Use Change (iLUC) factor. A comprehensive study to this point can be found in [6, 9]. However, [6] shows the expected development of CO₂ emission reduction by 2050, considering various influencing factors such as technology, operations and infrastructure, and SAF. The finding is that even in a technology-driven scenario, SAF will play a major role (Figure 1).

2. Methodology

This study takes up the potential of DHEP and SAF operation, introducing an on-design approach for hybrid electric powertrains of mid-range aircraft to address the challenges of future aviation. The design approach relies on the 0D-in-house tool ASTOR ([10, 11]) for the thermodynamic cycle performance calculation of gas turbines. It has been adapted for on-design calculation and extended by a DHEP model and a combustion chamber model to consider the combustion process and chemical emissions of SAFs in the design process of various hybrid electric powertrain concepts.

2.1 On-Design Analysis for DHEP systems

The overarching goal of an on-design analysis study is the identification of suitable design parameters in order to optimize the hybrid electric powertrain at given ambient conditions regarding predefined criteria. In order to conduct such a study for a DHEP system, an interdisciplinary analysis of the different components is necessary, particularly due to the incorporation of electrical machines. Therefore, the on-design analysis is split into separate modules that include the propeller modelling, the electrical system and the gas turbine design. The different modules are set up to depict a large variety of possible hybrid electric powertrain configurations. In that manner the on-design analysis is able to cover different DHEP architectures i.e. serial- or parallel configurations as well as different numbers and types of propellers, consisting of a turboprop and electrically driven propellers on the wing. The primary focus of the design process presented in this study is the evaluation of gas turbine designs with a special emphasis on the evaluation of emission products.

As the first step of the design process, the design point consisting of altitude and flight speed as well as the thrust demand for the whole DHEP system are selected from a reference mission. The thrust demand is distributed over the propellers, whereby the overall thrust is split between the electrically driven propellers and the turboprop by the split factor ρ_{TP} . Subsequently, the aerodynamic efficiency of each propeller is determined by a blade element momentum theory (BEMT) method [12]. The propeller efficiencies are used to convert the propulsion power demand to the shaft power demands at each propeller.

In the next step, the shaft power demand of the electrically driven propellers is converted to an electrical power demand, using the component efficiencies of the electric motors, the generator, as well as the power management and distribution system (PMAD). At this stage, the overall electric power demand as well as the turboprop shaft power is known and a hybridisation split between the battery and the gas turbine is determined by the hybridisation factor $H_{\rm B}$. Subsequently, the gas turbine power demand can be calculated.

Finally, an analysis of the gas turbine design at given ambient conditions is carried out based on the previously determined power requirement of the gas turbine. Thereby a Design of Experiments (DoE) study is conducted to analyse the performance of various gas turbine designs with different combinations of component parameters.

2.2 Combustion Modelling

The combustion chamber of the gas turbine is modelled based on two approaches for the combustion process. The first method is a 0D-chemical equilibrium approach (CE) utilizing the EB-SILON®Professional 16.1.0.33123 tool. The second method employs a simplified 0D-chemical reaction network approach (CRN) generated with the open-source tool Cantera 3.0.0 [13] and following a similar approach as in [14]. Both models constitute a strongly idealised representation of the combustion chamber which completely removes any geometrical information by dividing the flame tube

into three control volumes or zones, corresponding to a primary, secondary and dilution zone of a typical Rich-Burn, Quick-Mix, Lean-Burn (RQL)-type combustor. The combustion physics within these control volumes are calculated based on the mentioned approaches:

- 1. 0D-Chemical equilibrium: This modelling approach calculates the equilibrium composition in all three control volumes by minimising the Gibbs energy of the reaction system.
- 2. 0D-Chemical reaction network: The chemical reaction network approach is deployed assuming that all three zones (primary, secondary and dilution) can be approximated by means of Perfectly Stirred Reactors. The conservation equations for all species involved in the appropriate reaction mechanis are solved in an unsteady manner, allowing for state changes due to chemical reactions, while thermodynamic equilibrium is assumed throughout the reactor at all times. In the present study two mechanisms [15, 16] are adopted to describe the chemistry for standard Jet-A1 [17] and Jet-C1 SAF [16]. Both mecahnisms also account for NOx chemistry.

3. Model of the Hybrid Electric Powertrain: On-Design Analysis

As described in the previous section, the on-design analysis of the hybrid electric powertrain model consists of various sub-modules (Figure 2). The DHEP module considers the performance of electrical components for different hybrid electric concepts and is linked to a BEMT tool to consider the propeller performance (Subsection 3.1). The DHEP module provides the boundary conditions for the gas turbine module (Subsection 3.2). A combustion chamber module (Subsection 3.3) is integrated into the gas turbine module, both combined enable to determine the emissions for SAF as well as the performance data of the gas turbine. These modules as well as the setup of a DoE based on-design analysis study (Subsection 3.4) are described in greater detail in the following subsections.

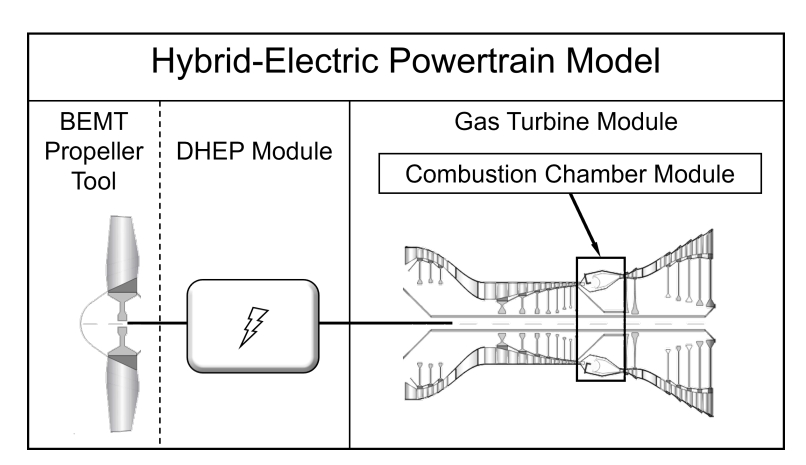


Figure 2 – Structure of the hybrid electric powertrain Model (adapted from [18]).

3.1 Distributed Hybrid Electric Propulsion and Propeller Module

In Figure 3 the structure of the DHEP module is shown. On an abstracted level, the most general type of hybrid electric powertrain is the serial/parallel partial hybrid architecture, which includes other architectures such as parallel or serial as limit cases as shown by [19] and is therefore selected as the model architecture. The DHEP system consists of a turboprop (TP) and several electrically driven propellers (EP). Thereby, the number of EPs $n_{\rm EP}$ can be defined in principle within an arbitrary range, the TP can either be included ($n_{\rm TP}=1$) or not ($n_{\rm TP}=0$). Several different architectures ranging from conventional turboprops, over parallel or serial hybrid systems to fully electric propulsion can be modeled in principle.

The thrust split between the electrically driven propellers and the turboprop is defined by the factor ρ_T .

$$\rho_{\rm TP} = \frac{T_{\rm TP}}{T_{\rm mission}} \text{ with } T_{\rm mission} = n_{\rm TP} T_{\rm TP} + n_{\rm EP} T_{\rm EP} \tag{1}$$

Thereby, $T_{\rm TP}$ denotes the thrust produced by the turboprop and $T_{\rm EP}$ is the thrust produced by a single electrically driven wing propeller. The upper and lower boundaries of the propeller diameters can

be derived by geometrical constraints that are given by the wingspan as well as minimum margins between the propellers. Based on the thrust demands, the ambient conditions, and the geometrical constraints, a propeller geometry is designed for each propeller type using the BEMT tool of [12]. The propeller performance maps are also calculated using the same BEMT tool. Subsequently, the shaft power demands of the gas turbine $P_{\rm GT}$ and each electric motor $P_{\rm EP}$ are calculated via the propeller efficiencies η_P from the propeller performance maps.

The sum of all propeller shaft powers P_{mission} can be expressed by the shaft power demands of the electrically driven wing propellers P_{EP} and the turboprop P_{TP} via Equation 2.

$$P_{\text{mission}} = n_{\text{EP}} P_{\text{EP}} + n_{\text{TP}} P_{\text{TP}} \tag{2}$$

The power conversion via the electric motors (EM), the power management and distribution system (PMAD), the electric generator (EG), and the gearbox (GB) is modelled using an estimate for each components efficiency taken from the literature (Table 4). Depending on the chosen DHEP architecture and a maximum power constraint for the battery, the sign of the power flow between GB and EM/EG $P_{\rm EM/EG}$ is decided. If the power is transferred from the PMAD to the GT, i.e., if the electrical system supports the GT, the value of $P_{\rm EM/EG}$ is positive. The overall power demand of the electrical system $P_{\rm EM}$ and the gas turbine power demand $P_{\rm GT}$ can be expressed via Equations 3 and 4.

$$P_{\rm E} = \eta_{\rm PMAD}(\eta_{\rm EM}(n_{\rm EP}P_{\rm EP}) + P_{\rm EM/EG}) \tag{3}$$

$$P_{\rm GT} = \eta_{\rm GB}(P_{\rm TP} - \eta_{\rm EM/EG}P_{\rm EM/EG}) \tag{4}$$

The level of hybridisation $H_{\rm B}$ is defined by Equation 5.

$$H_{\rm B} = \frac{P_{\rm E}}{P_{\rm DHEP}} \text{ with } P_{\rm DHEP} = P_{\rm E} + P_{\rm GT}$$
 (5)

According to a choosen hybridisation strategy, the value of $H_{\rm B}$ can be varied over a mission. Using Equations 3, 4 and 1 in combination with Equations 5 and 2, the gas turbine power demand $P_{\rm GT}$ can be calculated for a given $H_{\rm B}$.

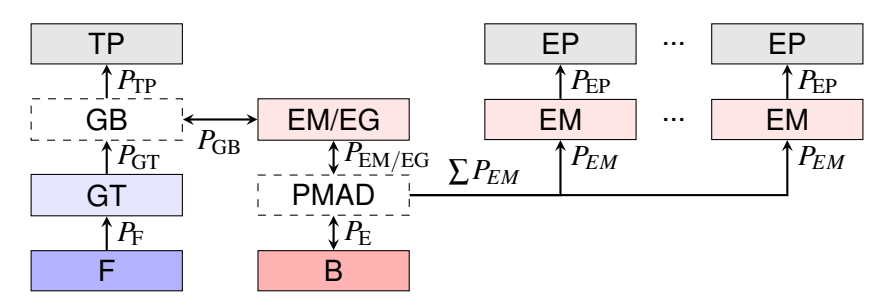


Figure 3 – Set up of the DHEP module.

3.2 Gas Turbine Module

The on-design performance analysis of the gas turbine is conducted by using the in-house tool AS-TOR. ASTOR is implemented in MATLAB/-Simulink 2019 [20, 21, 22]. Figure 4 shows the iteration scheme used in the gas turbine design module. Thereby, a set of component parameters together with the ambient conditions and the shaft power demand $P_{\rm GT}$, given by the design point and the hybridisation level, are used as input data. Within the cycle calculation, the thermodynamic properties of the fluid are determined at each station of the gas turbine. The component parameters consist of the compressor pressure ratio π_C , the combustor outlet total temperature $T_{\rm t,4}$ as well as the efficiency of the compressor $\eta_{\rm C}$ and the turbine $\eta_{\rm T}$. At this preliminary gas turbine design stage, the combustion and the expansion are each considered to take place within a single component, in order to evaluate the thermodynamic cycle with defined isentropic efficiencies. Further on in the design process, the compression and expansion can be split over several compressors and turbines. The compressor power $P_{\rm C}$ is calculated based on the enthalpy increase due to the given π_C . The overall fuel-to-air

ratio at the end of the combustor FAR_4 is determined using the integrated combustor model in order to optain the predefined $T_{t,4}$ value. The gas expansion within the turbine is maximised, resulting in a minimal thrust contribution due to the impulse increase in the core mass flow. Thereby, a minimum pressure ratio of 1.1 within the nozzle is assumed to ensure the core mass flow exhaust [23]. Using this constraint, the turbine pressure ratio is calculated, from which the turbine power $P_{\rm T}$ is calculated using the enthalpy difference due to the pressure decrease. The shaft power output of the gas turbine is calculated by Equation 6 from the power balance on the gas turbine spool.

$$P_{\text{shaft}} = P_{\text{T}} - P_{\text{C}} \tag{6}$$

Within the iterative design process, starting from an initial guess, the inlet mass flow \dot{m}_0 is varied using a Newton-Raphson method so that the residuum $|P_{\rm GT}-P_{\rm shaft}|$ is less than the given tolerance ε .

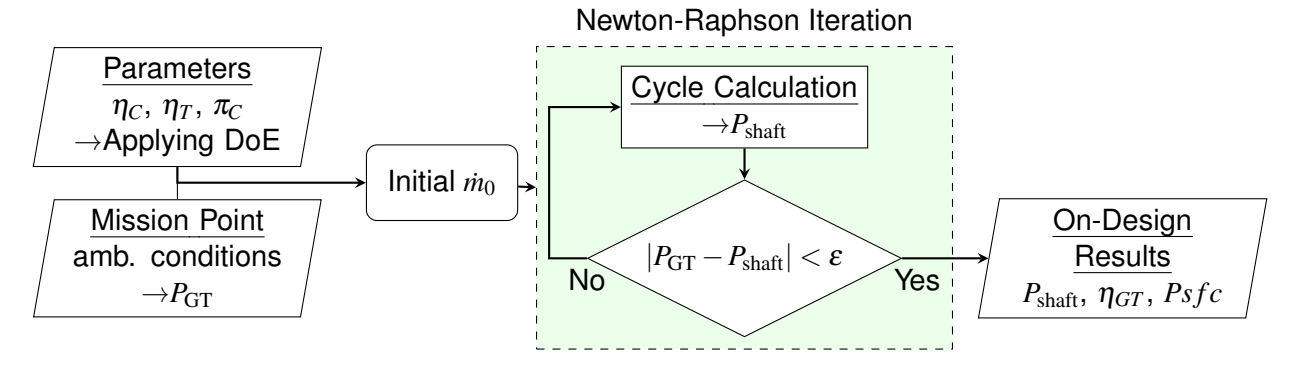


Figure 4 – Gas turbine on-desgin cycle calculation module.

3.3 Combustion Chamber Module

The combustion chamber follows the Rich-Burn, Quick-Mix, Lean-Burn (RQL) concept used in modern aircraft gas turbines to reduce NO_x , CO and UHC emissions. To incorporate the RQL concept into the modeling of the combustion chamber, the flame tube geometry is divided into three zones: the primary zone (PZ), the secondary zone (SZ) and the dilution zone (DZ) (Figure 5, left). In the primary zone, the fuel is rich-burned with an initial fraction of the total air mass flow supplied by the compressor to ensure a stable combustion process. The mixture then enters the secondary zone where it is mixed with an additional fraction of air and cooled - referred to as quenching - to reduce the NO_x production rate. Finally, in the dilution zone, the remaining air mass flow is added to produce a lean mixture in which partially oxidised hydrocarbons are further oxidised to reduce the NO_x , CO and UHC production.

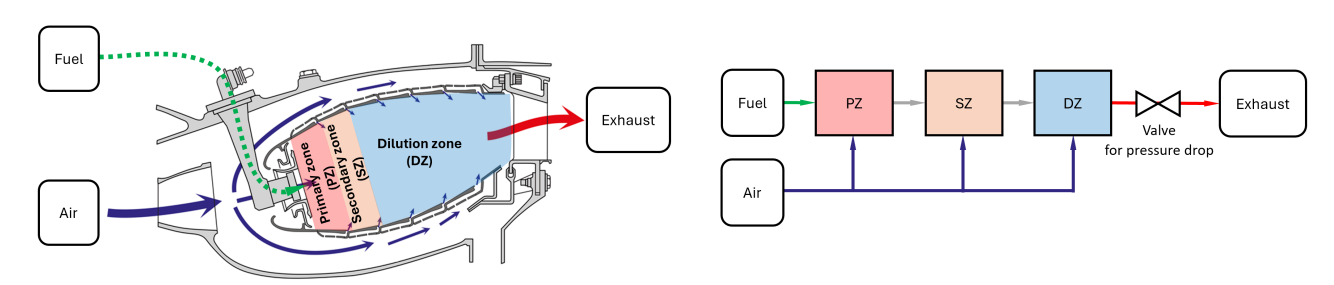


Figure 5 – Schematic of combustion chamber cross section (left, adapted from [24]) and abstracted combustor model (right).

These zones are modelled by reactor components that are connected by mass flows with corresponding gas properties and composition (Figure 5, right). Gibbs reactors for the CE model and perfectly stirred reactors for the CRN model are utilized. Additional components included are reservoirs, which represent infinitely large volumes, ensuring air and fuel mass flow supply for the reactors with constant gas properties and composition. The air mass flow is distributed to the reactors based on the

factor A_i ($i = \{PZ, SZ, DZ\}$), listed in Table 2. A third reservoir, the exhaust, absorbs the exhaust gas after the combustion chamber or dilution zone, respectively. Here, a valve component allows accounting for the specific relative pressure loss of the combustion chamber $\Delta p_{\%}$. In case of the CE model, reservoirs are not considered. Instead, inlet conditions for the air and fuel mass flow are specified directly at the inlet of the reactors, and the exhaust gas after the valve is released into the environment.

In the case of the CRN model, the combustion process must be ignited. This is achieved by setting the initial value of the temperature in the first reactor (PZ) to be sufficiently high to ignite the air-fuel mixture. The combustion reactions in the subsequent reactors (SZ and DL) are then started by the combustion gas produced in the PZ reactor. An alternative common ignition method is to inject a brief, pulsed mass flow of reactive hydrogen into the first reactor (PZ). This method requires a sufficiently large mass flow to generate enough heat for ignition. However, too high a mass flow significantly affects the combustion reactions and, therefore, the combustion product composition. This dilemma requires an iterative approach to determine just enough hydrogen mass flow for ignition. Since a large number and wide range of operating points are calculated for the lookup table creation, the iterative method is not practicable. Therefore, to start the combustion process, the ignition method with an initial temperature of 1900 K is used.

3.3.1 Validation of the Combustion Chamber Models

To validate the combustion chamber models created, the calculated emission products for four different operating scenarios (take-off, climb, approach, idle) were compared with data from the ICAO databank [25]. The ICAO databank contains information on the exhaust emissions of certified turbofan and turbojet engines of production aircraft according to a standardized procedure. For the validation purpose, the data of the CFM56-7B27 engine, a two-spool high-bypass turbofan engine, were used. The required geometry data and operating conditions of the combustion chamber were prepared on the basis of [14] and are summarized in Table 2.

Table 2 – 0	Operating	points ar	nd data fo	or the con	nbustion	chamber	models
Tubic 2	Jpciani g	points at	ia aata k	, ,,,,	ibastion	CHAILIDCI	modelo.

	Operating Scenarios				
	Take-off	Climb	Approach	ldle	
Power Setting in %	100	85	30	7	
$T_{t,in}$ in K	795	759	619	477	
\dot{m}_{air} in kg/s	47.47	42.8	21.33	8.32	
FAR (AFR)	0.026 (38.46)	0.024 (41.67)	0.016 (62.5)	0.014 (71.43)	
A_{PZ} in %	0.3082				
A_{SZ} in %	0.2302				
A_{DZ} in %	0.4616				
V_{PZ} in m^3	0.007037				
V_{SZ} in m^3	0.006882				
V_{DZ} in m^3		0.020	801		
$\Delta p_\%$ in %	5.01				

The inlet conditions of the combustion chamber are defined by the pressure $p_{t,in}$, the temperature $T_{t,in}$, and the air mass flow rate \dot{m}_{air} . The fuel mass flow rate is determined by the fuel-to-air ratio (FAR) or air-to-fuel ratio (AFR), respectively. The air mass flow rate \dot{m}_{air} is distributed to each zone of the combustion chamber or reactors by the factors A_i . This distribution can be reasonably assumed to be constant for all operating scenarios considered. In case of the CRN model, the volumes of each combustion chamber zones V_i have to be defined, which influence the residence time of the combustion gas in the zones and thus the emission products of the exhaust gas. For the modelling of kinetic reaction mechanisms, the model of [15] is applied and the jet fuel is defined by the surrogate composition according to [17], i.e., n-propylbenzene (PHC3H7 = 15 %), n-Decane (NC10H22 = 74 %), n-propylcyclohexane (CYC9H18 = 11 %) (mole fractions).

Figure 6 shows the results of the combustion models as emission indices EI for nitrogen oxides

-ICAO ICAO -ICAO CRN model CRN model CRN model $\mathrm{EI}_{\mathrm{NOx}}$ in g/(kg fuel) EI UHC in g/(kg fuel) in g/(kg fuel) 15 1.5 CE model 40 EI_{CO} i 0 ┗ 100 00-40 20 80 60 100 60 60 40 80 40 Power Setting in % Power Setting in % Power Setting in %

Figure 6 – Results of CE and CRN model compared with ICAO data.

 $(NO_x = NO + NO_2)$, carbon monoxide (CO) and unburned hydrocarbons (UHC) for the four operating scenarios of the engine. The operating scenarios are characterised by their relative power in respect of the maximum power during take-off, known as the power setting values: 100 % (take-off), 85 % (climb), 30 % (approach) and 7 % (idle).

The CE model is unable to predict UHC and CO emissions accurately. While it can reproduce the trend for NO_x emissions, there are significant deviations—by a factor of about 2.5—during the take-off (100 %) and climb (85 %) operating scenarios. This discrepancy arises because the CE model assumes an infinitely long residence time for the combustion gases in the primary zone, leading to increased NO_x generation. In contrast, the CRN model, which accounts for the residence time, shows satisfactory agreement with ICAO validation data for both NO_x and CO emissions. However, it predicts significantly lower UHC emissions, despite qualitatively reproducing the trend of increasing UHC emissions for operating scenarios with lower power demands (approach and idle). Compared to the results of [14], who also adopted a CRN model with three reactors, the present approach shows satisfactory agreement. Overall, the CRN model provides a solid basis for realistically determining combustion chamber emissions and for subsequent work steps.

3.3.2 Integration of the Combustor Module into the Gas Turbine Module

The combustion chamber module created is integrated into the gas turbine module utilising lookup tables. This enables an efficient and versatile integration of combustion models of any complexity. The lookup table contains only intensive variables, ensuring that the combustion chamber model is independent of the gas turbine size. The input variables for the lookup table are the Air-to-Fuel Ratio (AFR) or Fuel-to-Air Ratio (FAR) and the combustion chamber inlet temperature $T_{t,3}$. The combustion process is assumed to be isobaric, with the result that pressure is not included as an input variable. The combustion chamber outlet temperature $T_{t,4}$ is determined by solving the energy equation for the combustion chamber model. The results for $T_{t,4}$ are also integrated into the lookup table, enabling the determination of the combustion chamber outlet temperature $T_{t,4}$ by a fast bi-linear interpolation without having to solve the energy equation in the hybrid electric powertrain model. The mass concentrations of all combustion products are also included in the lookup table, allowing the determination of the emission profile at the combustion chamber outlet. A second lookup table, constructed in the same way, is used to describe the state properties of the exhaust gas (FAR > 0) and the air (FAR = 0) according to [26] at any position within the gas turbine.

3.4 Design of Experiments Study and Constraints

The on-design analysis process described in this study is set up to cover a broad parameter space. To demonstrate the functionality of the design process, a set of constraints is defined within this study to serve as an example case. Thus, a parallel hybrid electric powertrain architecture is considered that incorporates one turboprop and five electrically driven wing propellers. The design point conditions are derived from a reference mission of an ATR-72 turboprop aircraft [27] at take-off, as given in Table 3. The efficiencies of the electrical components and the gearbox are taken from the literature, while the efficiency of the turbo components is based on experience. A summary of all efficiency values is shown in Table 4.

The level of hybridisation determines the power requirements of the gas turbine as well as the electric system. Due to the low power and energy density of batteries compared to combustion fuel, the

Table 3 – Altitude, flight speed, and thrust at take-off conditions.

H in m	V in m/s	$T_{ m mission}$ in kN	
0	60	68.37	

Table 4 – Assumed component efficiencies.

Component	Efficiency in %	Source	
Electric Motor	95	[28]	
PMAD	97	[29]	
Gearbox	98	[30]	
Compressor	80		
Turbine	85		

overall weight of the propulsion system increases significantly with an increasing hybridisation factor, either increasing the maximum take-off weight or decreasing the payload weight. Therefore, the additional weight due to the electric system constrains the maximum level of hybridisation. For the purpose of this study, an exemplary level of hybridisation of $H_{\rm B}=0.5$ is selected. According to [28], to achieve that level of hybridisation in an aircraft design using the top level requirements of an ATR-72, the battery mass reaches approximately 3000 kg.

The CRN model is used for the combustion chamber. To account for the properties and chemical reactions of SAF, the chemical reaction network model from [16] for Jet-C1 fuel, an AtJ fuel, with NO chemistry is employed.

In order to identify suitable gas turbine design parameters, a design of experiments (DoE) is applied, using a latin hypercube sampling method to vary π_C and $T_{t,4}$. A summary of the DoE parameter ranges is shown in Table 5.

Table 5 – Design of Experiments parameter ranges.

Parameter	Range		
$\pi_{ m C}$	[10 - 40]		
$T_{t,4}$ in K	[1500 - 2000]		

4. Results and Discussion

To select a suitable gas turbine design for the hybrid electric powertrain model, the emission production for each component parameter combination of $\pi_{\mathbb{C}}$ and $T_{t,4}$ from the DoE study is evaluated. This evaluation considers emission indices EI as well as the power-specific fuel consumption PSFC. Additionally, the weight of the gas turbine needs to be considered for an overall evaluation of the design. Figure 7 shows the DoE results based on the compressor performance map, whereby each circle represents a distinct combination of $\pi_{\mathbb{C}}$ and $T_{t,4}$. In the left chart, the scatter colour shows the CO emission index EI_{CO} , while in the right chart, PSFC is represented in the scatter colour. These results are discussed in the following for demonstration purposes for a possible design selection. All DoE samples depicted as circles in Figure 7 meet the power requirements specified within the DoE for the hybrid electric powertrain, considering state-of-the-art gas turbine constraints, thus representing feasible designs in principle. However, to reduce CO emissions (Figure 7, left), the combustion

for the hybrid electric powertrain, considering state-of-the-art gas turbine constraints, thus representing feasible designs in principle. However, to reduce CO emissions (Figure 7, left), the combustion chamber outlet or turbine inlet temperature should be kept below approximately 1700 K. In addition, above 1700 K, the sensitivity of CO emission in regards the $\pi_{\rm C}$ increase, whereby higher $\pi_{\rm C}$ leads to a reduction in CO emissions. Nevertheless, the most effective way to reduce CO emissions is to lower the turbine inlet temperature. Unfortunately, reducing the temperature results in higher corrected and therefore absolute mass flow rates of the compressor, leading to larger and heavier gas turbine designs; an aspect that is particularly crucial for hybrid electric aircraft. (The corrected and absolute mass flow rates are nearly identical, as the temperature and pressure conditions at the engine intake for take-off are the same as those used for the corrected values).

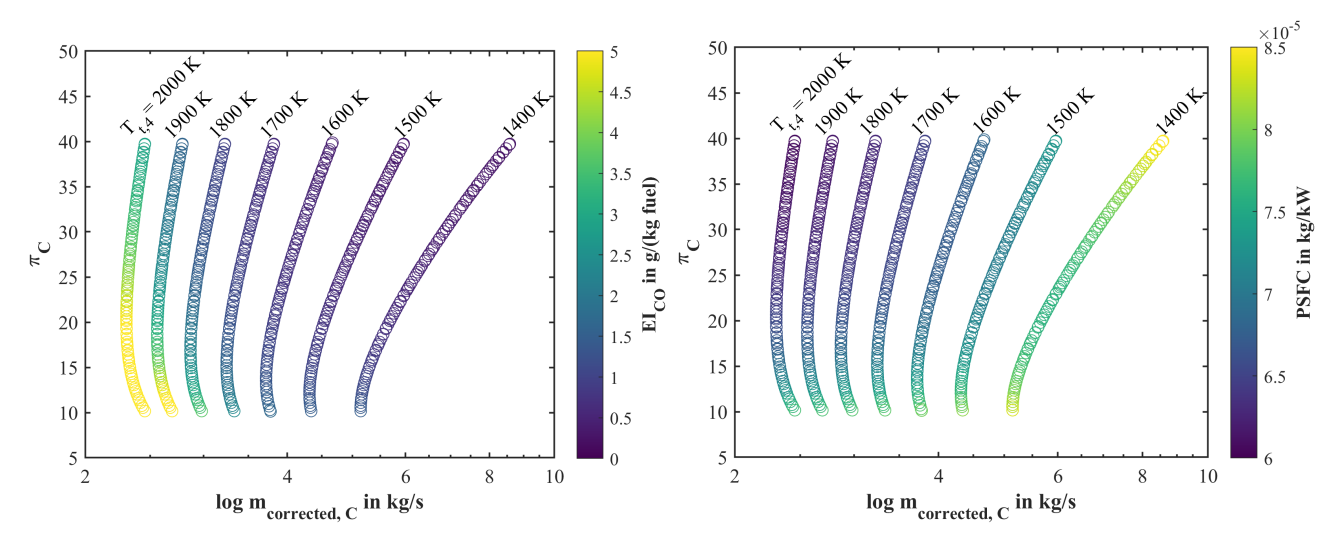


Figure 7 – Relationship between compressor pressure ratio, corrected mass flow rate of the compressor, inlet temperature of the turbine vs. EI_{CO} (left) and PSFC (right).

Therefore, a suitable design, driven by CO emission reduction, could be at a turbine inlet temperature of approximately 1500 K, with the lowest mass flow rate at an $\pi_{\rm C}$ value of about 15. The use of state-of-the-art materials in today's high-pressure turbines for turboprops allows temperatures of up to about 1500 K to be realised without the need for additional cooling [31]. Furthermore, lower $\pi_{\rm C}$ values require fewer compressor and turbine stages. Both have a positive effect on the size and weight of the gas turbine.

With additional consideration of the PSFC (Figure 7, right), it is evident that the fuel consumption per unit of power decreases with increasing $T_{t,4}$, and also, but less significantly, with higher π_C . This leads to lower absolute emissions of CO and other pollutants. However, the indirect influence of an increase in $T_{t,4}$ on the reduction of CO emissions through PSFC is significantly lower than the direct influence on the increase in EI_{CO} . Consequently, maintaining $T_{t,4}$ at lower levels, such as the 1500 K mentioned above, seems to be the preferred option, especially when the cooling aspect is also considered. Nonetheless, a slight increase in π_C from 15 to approximately 20 to 25 could further reduce CO emissions and PSFC. However, this needs to be balanced with the increase in size and weight of the gas turbine due to slightly higher mass flow rates.

5. Conclusion and Outlook

The present study introduces an on-design approach for future hybrid electric propeller propulsion systems for mid-range aircraft. This approach aims to meet the ambitious goals of reducing CO_2 emissions by 75 %, NO_x emissions by 90 %, and noise emissions by 65 % until 2050, as outlined by the Flightpath 2050 agenda ([1, 2]) set by policymakers and the aerospace industry. The current design approach considers various propulsion system architectures, ranging from conventional turbo-props and parallel or serial hybrid electric systems to fully-electric propulsion as well as combustion emissions of SAF. For this purpose, the 0D in-house tool ASTOR ([10, 11]), used for thermodynamic cycle performance calculation of gas turbines, was extended by a DHEP model in combination with a BEMT propeller model by [12] and a combustion chamber model. This extension takes into account the performance of the combustion, gas turbine, propeller, and electrical components. For the combustion chamber, a CRN model has proven suitable for considering NO_x and CO emissions, with potential for improvements in UHC emissions.

To demonstrate the capabilities of the on-design approach, a DoE-based design process was conducted for a parallel hybrid electric powertrain architecture considering one turboprop and five electrically driven wing propellers for take-off condition. For this, a reference mission of an ATR-72 aircraft was selected. Results were discussed in terms of CO emissions reduction, *PSFC* reduction, and potential design selections. The main findings are:

1. CO emission: keeping the turbine inlet temperature below 1700 K minimizes CO emissions

significantly. An increase in $\pi_{\mathbb{C}}$ values also helps reduce CO emissions, but lowering the temperature is more effective. However, a reduction in temperature leads to an increase in turbine size and weight due to higher mass flow rates.

2. PSFC: PSFC decreases with higher $T_{t,4}$ with an indirect effect of lower CO and other emissions. However, lowering $T_{t,4}$ to 1500 K is preferable as it reduces CO emissions more effectively. Increasing $\pi_{\rm C}$ slightly (to 20-25) can further reduce CO emissions and PSFC.

In summary, in terms of reducing CO emissions and PSFC appropriate design parameters seem to be a turbine inlet temperature of around 1500 K and an π_C of about 15 to slightly higher values up to 25. This setup meets CO emissions at relatively low PSFC and avoids the need for additional cooling, potentially reducing the number of compressor and turbine stages and therefore the size and weight of the gas turbine.

Future work will focus on several points:

- The flexible integration of combustion chamber models through lookup tables allows for the integration of more complex reduced combustion chamber models based on data of high-fidelity Computational Fluid Dynamics (CFD) simulations to enhance prediction accuracy of emissions from SAF.
- 2. The powertrain model will be extended by a propeller acoustic model to account for noise emissions during the design process and to address noise emission goals.
- 3. Development of an off-design powertrain model to evaluate emission and performance parameters for cruise conditions within the on-design process and additionally for a complete flight mission.

6. Acknowledgment

The authors gratefully acknowledge Mr. Jan Donndorf from the EU Horizon Project MYTHOS for his insightful discussions on combustion.

This study is conducted as part of the Horizon Europe research programme. The study is supported by the European Climate, Infrastructure and Environment Executive Agency (CINEA) under grant number 101096055.

7. Contact Author Email Address

karl.ziaja@rub.de

8. Copyright Statement

The authors confirm that they, and/or their company or organization, hold copyright on all of the original material included in this paper. The authors also confirm that they have obtained permission, from the copyright holder of any third party material included in this paper, to publish it as part of their paper. The authors confirm that they give permission, or have obtained permission from the copyright holder of this paper, for the publication and distribution of this paper as part of the ICAS proceedings or as individual off-prints from the proceedings.

References

- [1] D.S. Lee, D.W. Fahey, A. Skowron, M.R. Allen, U. Burkhardt, Q. Chen, S.J. Doherty, S. Freeman, P.M. Forster, J. Fuglestvedt, A. Gettelman, R.R. De León, L.L. Lim, M.T. Lund, R.J. Millar, B. Owen, J.E. Penner, G. Pitari, M.J. Prather, R. Sausen, and L.J. Wilcox. The contribution of global aviation to anthropogenic climate forcing for 2000 to 2018. Atmospheric Environment, 244:117834, 2021.
- [2] European Commission, Directorate-General for Mobility, Transport, Directorate-General for Research, and Innovation. Flightpath 2050 Europe's vision for aviation Maintaining global leadership and serving society's needs. Publications Office, 2011.
- [3] EUROCONTROL. Aviation outlook 2050. 2022.
- [4] Steven R. H. Barrett, Rex E. Britter, and Ian A. Waitz. Global mortality attributable to aircraft cruise emissions. Environmental Science & Technology, 44(19):7736–7742, 2010.
- [5] Ted Elliff, Michele Cremasci, Violaine Huck, and Paris Envisa. Impact of noise pollution on residents of large cities, with special regard to noise pollution from aircrafts. J. Eng. Gas Turbines Power, 2020.
- [6] Matteo Prussi, Uisung Lee, Michael Wang, Robert Malina, Hugo Valin, Farzad Taheripour, César Velarde, Mark D. Staples, Laura Lonza, and James I. Hileman. Corsia: The first internationally adopted approach to calculate life-cycle ghg emissions for aviation fuels. Renewable and Sustainable Energy Reviews, 150:111398, 2021.
- [7] European Environment Agency and European Union Aviation Safety Agency. <u>European aviation</u> environmental report 2022. Publications Office of the European Union, 2023.
- [8] Air Transport Action Group. Balancing growth in connectivity with a comprehensive global air transport response to the climate emergency: a vision of net-zero aviation by mid-century. Waypoint 2050 report, 2021.
- [9] V. Batteiger, K. Ebner, A. Habersetzer, and L. Moser. Power-to-liquids a scalable and sustainable fuel supply perspective for aviation. 2022.
- [10] J. Goeing, H. Seehausen, S. Lueck, J. Seume, and J. Friedrichs. Influence of combined compressor and turbine deterioration on the overall performance of a jet engine using rans simulation and pseudo bond graph approach. Journal of the Global Power and Propulsion Society 4, 2020.
- [11] L. Schuchard, M. Bień, K. Ziaja, N. Blanken, J. Goeing, J. Friedrichs, F. di Mare, B. Ponick, and R. Mailach. A study on quantities driving maintenance, repair, and overhaul for hybrid-electric aeroengines. <u>J. Eng. Gas Turbines Power</u>, 2024.
- [12] Sebastian Lück, Jan Göing, Tim Wittmann, Bastian Kirsch, Leroy Benjamin, and Jens Friedrichs. Propeller design and performance evaluation with partially prescribed velocity distribution. Proceedings of Global Power and Propulsion Society, page 2021, 2021.
- [13] David G. Goodwin, Harry K. Moffat, Ingmar Schoegl, Raymond L. Speth, and Bryan W. Weber. Cantera: An object-oriented software toolkit for chemical kinetics, thermodynamics, and transport processes. https://www.cantera.org, 2023. Version 3.0.0.
- [14] Sergios Villette, Dimitris Adam, Alexios Alexiou, Nikolaos Aretakis, and Konstantinos Mathioudakis. A simplified chemical reactor network approach for aeroengine combustion chamber modeling and preliminary design. Aerospace, 11(1), 2024.

- [15] J. Luche. Obtention de modeles cinetiques reduits de combustion: Application a un mecanisme du kerosene. PhD Thesis, Universite D'Orleans, 2003.
- [16] Ji-Woong Park, Rui Xum, Tianfeng Lu, and Hai Wang. Skeletal and reduced model of nox formation in c1 (gevo atj) synthetic jet fuel. 2019.
- [17] Quan-De Wang, Ya-Mei Fang, Fan Wang, and Xiang-Yuan Li. Skeletal mechanism generation for high-temperature oxidation of kerosene surrogates. Combustion and Flame, 159(1):91–102, 2012.
- [18] Joachim Kurzke. Fundamental Differences Between Conventional and Geared Turbofans. volume Volume 1: Aircraft Engine; Ceramics; Coal, Biomass and Alternative Fuels; Controls, Diagnostics and Instrumentation; Education; Electric Power; Awards and Honors of <u>Turbo Expo: Power for Land, Sea, and Air, pages 145–153</u>, 06 2009.
- [19] Reynard de Vries. Hybrid-electric aircraft with over-the-wing distributed propulsion: Aerodynamic performance and conceptual design, 2022.
- [20] Jan Goeing. <u>Modellierung des nicht-linearen aerothermodynmaischen Systemverhaltens von</u> Flugantrieben. PhD thesis, Technische Universitaet Braunschweig, 2023.
- [21] J. Goeing, H. Seehausen, L. Stania, N. Nuebel, J. Salomon, P. Ignatidis, F. Dinkelacker, M. Beer, B. Denkena, J. Seume, and J. Friedrichs. Virtual process for evaluating the influence of real combined module variations on the overall performance of an aircraft engine. <u>Journal of the Global Power and Propulsion Society</u>, 7:1–18, 2023.
- [22] J. Göing, J. Hogrefe, S. Lück, and J. Friedrichs. Validation of a dynamic simulation approach for transient performance using the example of a turbojet engine. pages 559–568, 2020.
- [23] Christopher A Snyder and Michael T Tong. Modeling turboshaft engines for the revolutionary vertical lift technology project. In <u>Annual Forum and Technology Display: The Future of Vertical Flight</u>, number GRC-E-DAA-TN66991, 2019.
- [24] Thomas Jackowski, Maximilian Elfner, Hans-Jörg Bauer, Katharina Stichling, and Marco Hahn. Experimental study of impingement effusion cooled double-wall combustor liners: Aerodynamic analysis with stereo-piv. Energies, 14(19), 2021.
- [25] European Union Aviation Safety Agency. Icao aircraft engine emissions databank. <u>Combustion and</u> Flame, 2023.
- [26] Bonnie J. McBride and Sanford Gordon. Computer program for calculation of complex chemical equilibrium compositions and applications ii. users manual and program description. 1996.
- [27] Benedict Jux, Simon Foitzik, and Martin Doppelbauer. A standard mission profile for hybrid-electric regional aircraft based on web flight data. In 2018 IEEE International Conference on Power Electronics, Drives and Energy Systems (PEDES), pages 1–6. IEEE, 2018.
- [28] Julian Hoelzen, Yaolong Liu, Boris Bensmann, Christopher Winnefeld, Ali Elham, Jens Friedrichs, and Richard Hanke-Rauschenbach. Conceptual design of operation strategies for hybrid electric aircraft. Energies, 11(1):217, 2018.
- [29] Gerald Brown. Weights and efficiencies of electric components of a turboelectric aircraft propulsion system. In 49th AIAA aerospace sciences meeting including the new horizons forum and aerospace exposition, page 225, 2011.
- [30] Neil E Anderson, Stuart H Loewenthal, and Joseph D Black. An analytical method to predict efficiency of aircraft gearboxes. 1986.
- [31] Willy J.G. Bräunling. Flugzeugtriebwerke, volume 4. Springer Vieweg Berlin, 2015.